Electronic Supplementary Material to: Superiority of a Convolutional Neural Network Model over Dynamical Models in Predicting Central Pacific ENSO*

Tingyu WANG[1,4] and Ping HUANG[1,2,3]

[1]*Center for Monsoon System Research*, *Institute of Atmospheric Physics*, *Chinese Academy of Sciences*, *Beijing* 100029, *China*

[2]*Collaborative Innovation Center on Forecast and Evaluation of Meteorological Disasters (CIC-FEMD)*, *Nanjing University of Information Science* & *Technology*, *Nanjing* 210044, *China*

[3]*State Key Laboratory of Numerical Modeling for Atmospheric Sciences and Geophysical Fluid Dynamics*, *Institute of Atmospheric Physics*, *Chinese Academy of Sciences*, *Beijing* 100029, *China*

[4]*University of Chinese Academy of Sciences*, *Beijing* 100049, *China*

ESM to: Wang, T. Y., and P. Huang, 2024: Superiority of convolutional neural network model over the dynamical models in predicting the central Pacific ENSO. *Adv. Atmos. Sci.*, **41**(1), 141−154, https://doi.org/10.1007/s00376-023-3001-1.

Text S1. Prediction skill for CP and EP ENSO

To evaluate the prediction skill for CP and EP ENSO, the CTI and WPI are used to represent the two types of ENSO following previous studies (Kug et al., 2009; Yeh et al., 2009; Ren and Jin, 2011; Takahashi et al., 2011; Sullivan et al., 2016; Freund et al., 2019; Wang et al., 2020):

$$\begin{cases} \mathrm{CTI} = N_3 - \alpha N_4 \\ \mathrm{WPI} = N_4 - \alpha N_3 \end{cases}, \quad \alpha = \begin{cases} 2/5, & N_3 N_4 > 0 \\ 0, & \text{otherwise} \end{cases},$$

where N_3 and N_4 denote the Niño-3 [averaged SSTAs in (5°S–5°N, 90°–150°W)] and Niño-4 [averaged SSTAs in (5°S–5°N, 160°E–150°W)] indices, respectively. The predictions for the period 1986–2019 are evaluated, whereas the datasets in the two years 1984 and 1985 are used to develop the fusion model.

Text S2. Discussion

ENSO diversity is shown in terms of spatial pattern, temporal evolution, and amplitude, so "no two El Niño events are quite alike" (Wyrtki, 1975), and no two El Niño precursors are the same. However, we can still conclude that the CNN model learned some useful signals, found by previous studies, in the initial-month SSTAs. A La Niña-like initial condition during the first decade of the 21st century is highlighted in Fig. S7, which is possibly conducive to the development of CP El Niño events in this period (Capotondi et al., 2020). Moreover, some signals can favor the development of EP El Niño, such as the western North Pacific cooling SSTAs in boreal winter (Wang et al., 2012) (Fig. S8) and the South Pacific Meridional Mode (Zhang et al., 2014) (Fig. S9).

*The online version of this article can be found at https://doi.org/10.1007/s00376-023-3001-1.

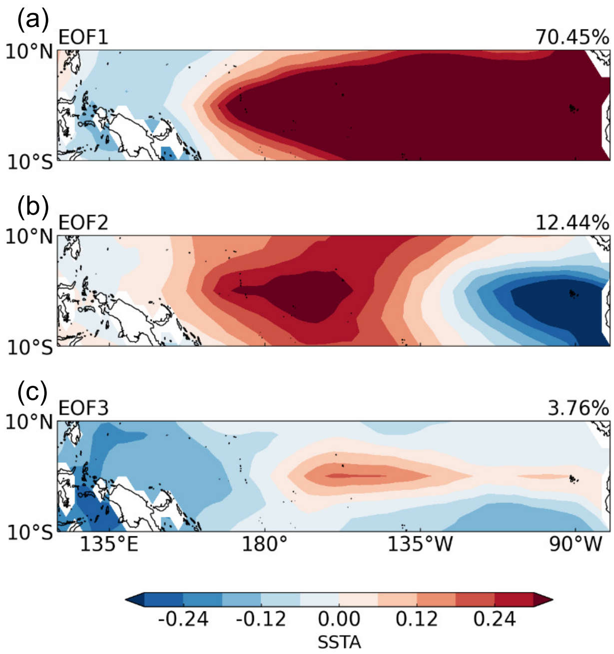

Fig. S1. EOF patterns of the equatorial Pacific: (a–c) three leading EOF modes of the equatorial Pacific for the period from 1960 to 1986. Upper-right value for each mode is the percentage of variance explained.

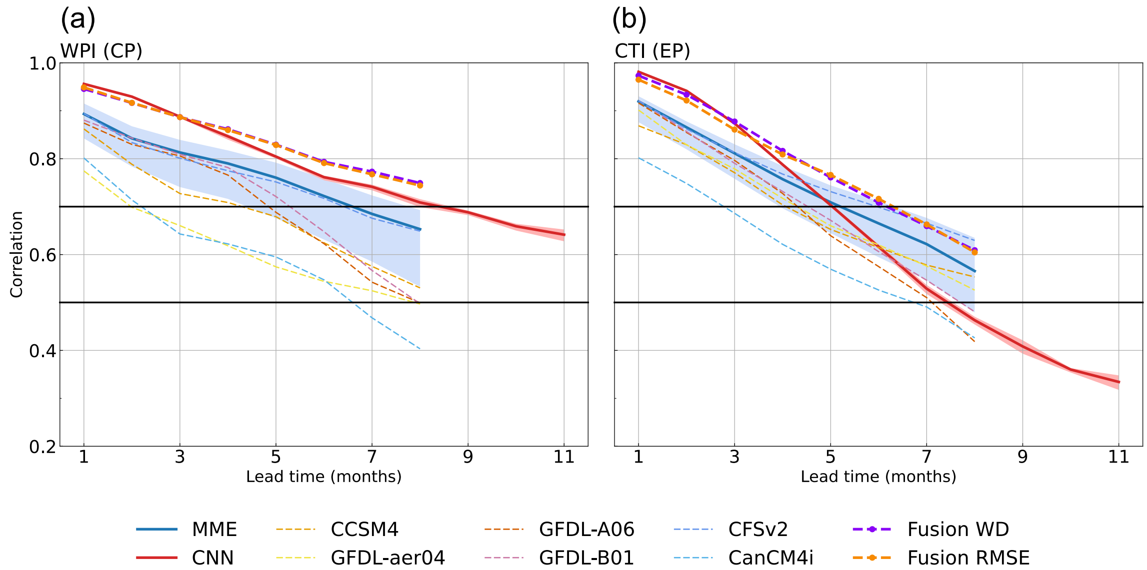

Fig. S2. All-season prediction skill for the two types of ENSO in the CNN model. As in Fig. 3 but for the MME including NCEP-CFSv2.

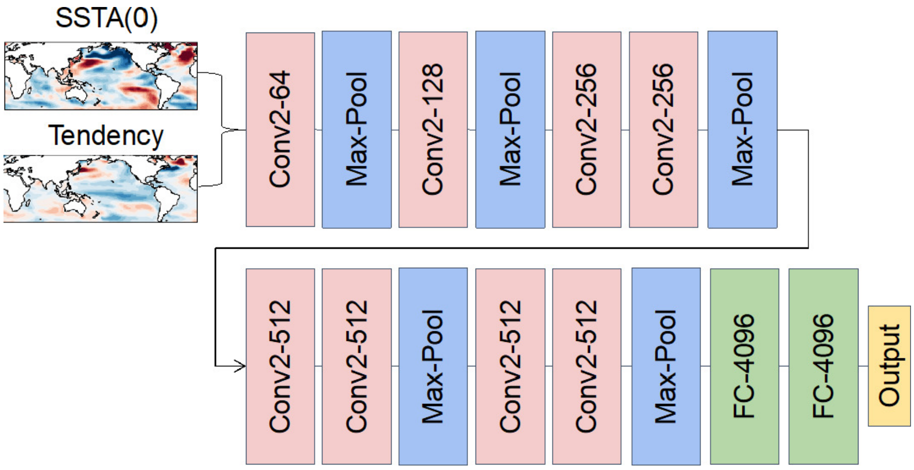

Fig. S3. Architecture of the VGG-11 model. Predictors are SSTA and SSTA tendency as two channel image–like input data. Convolutional layers are denoted by the red boxes, max-pooling layers by the blue boxes, and full connected layers by the green boxes. The output is one of the coefficients of the EOF modes at a certain lead time.

Fig. S4. Pattern correlation coefficients of the CNN model and the NMME model in predicting two types of ENSO with DJF as the target season at a lead time of 11 months.

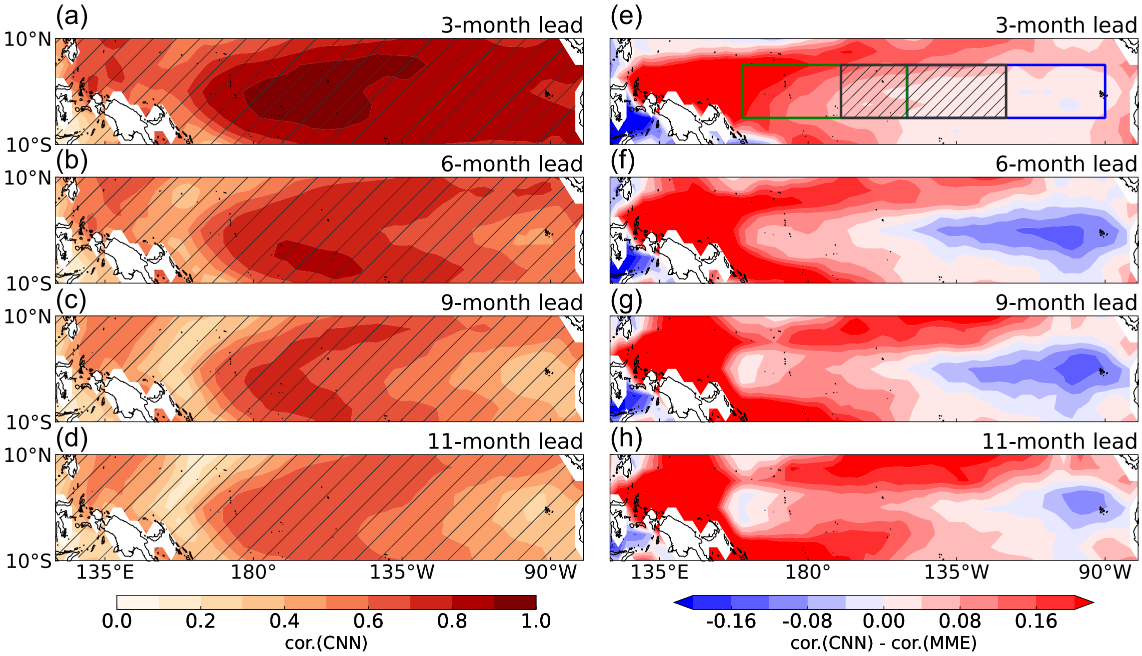

Fig. S5. Prediction skill for the SSTAs in the equatorial Pacific. As in Fig. 2 but removing the warming trend from dataset and prediction skill of the NMME model.

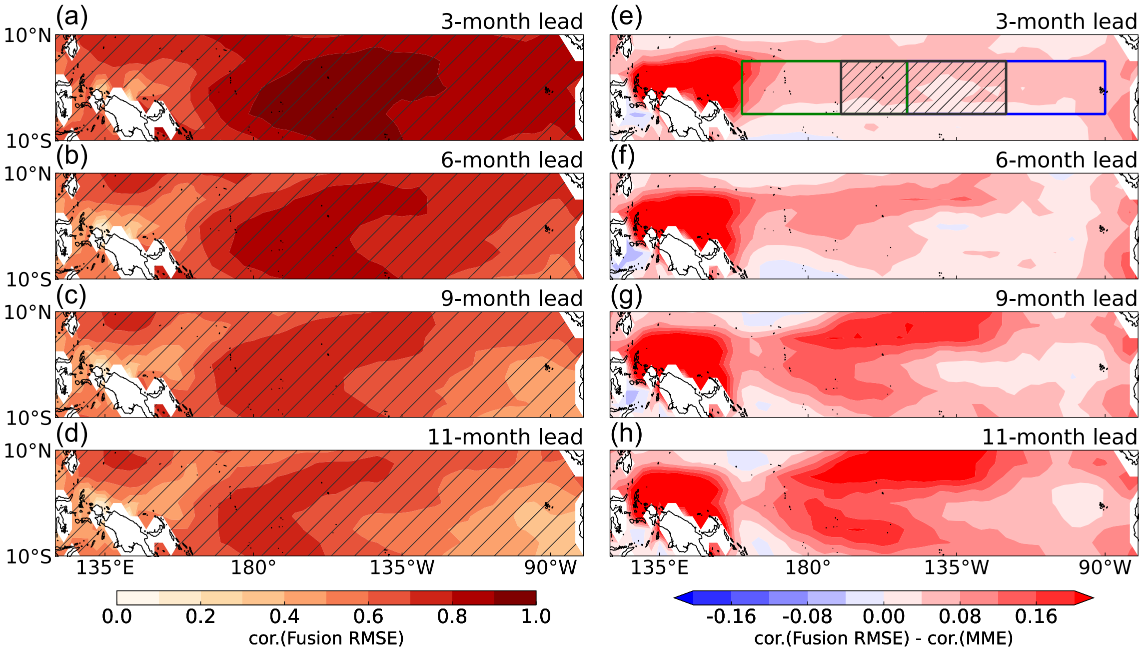

Fig. S6. As in Fig. 8 but for the prediction skill of the fusion model in which RMSE is used as the distance metric.

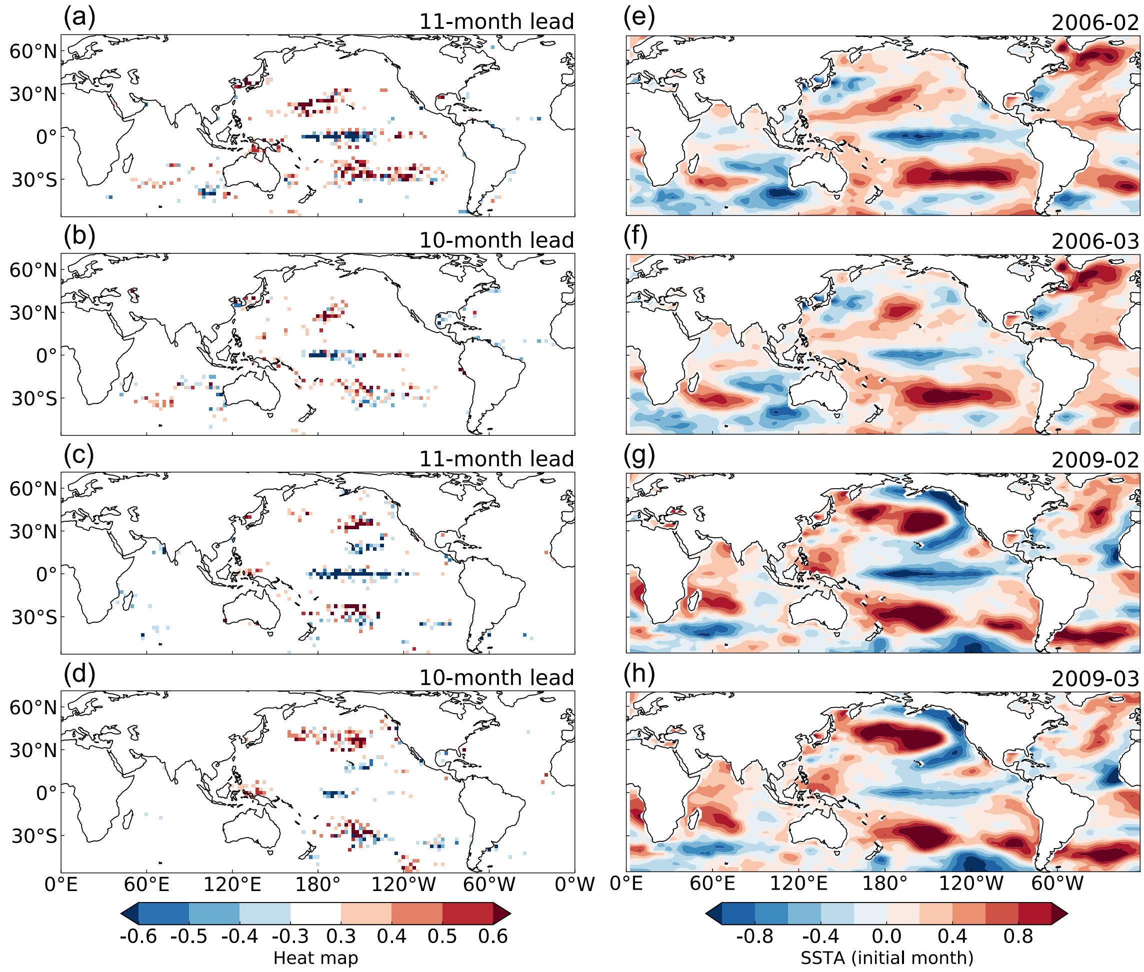

Fig. S7. Attribution heat map of CP El Niño in the 21st century.

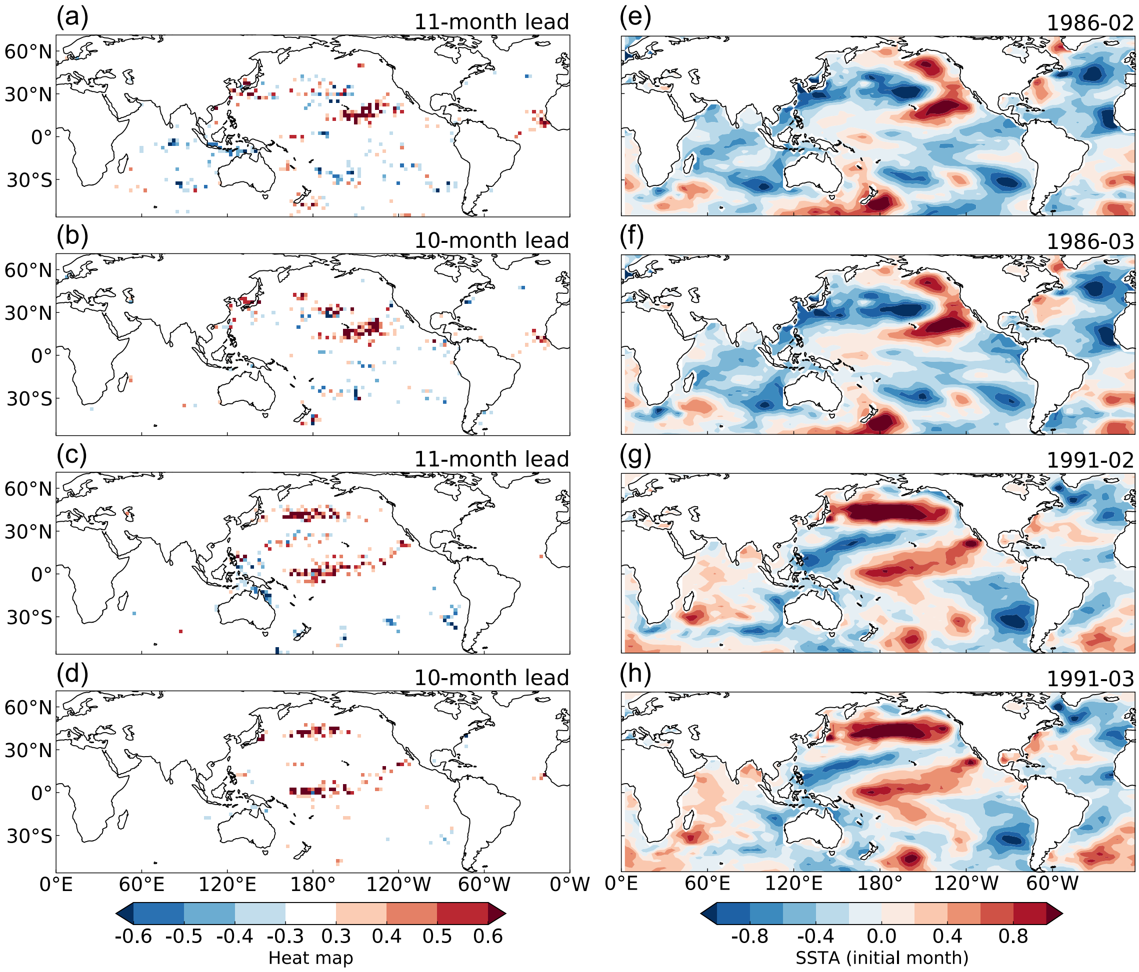

Fig. S8. Attribution heat map of EP El Niño in 1986 and 1991.

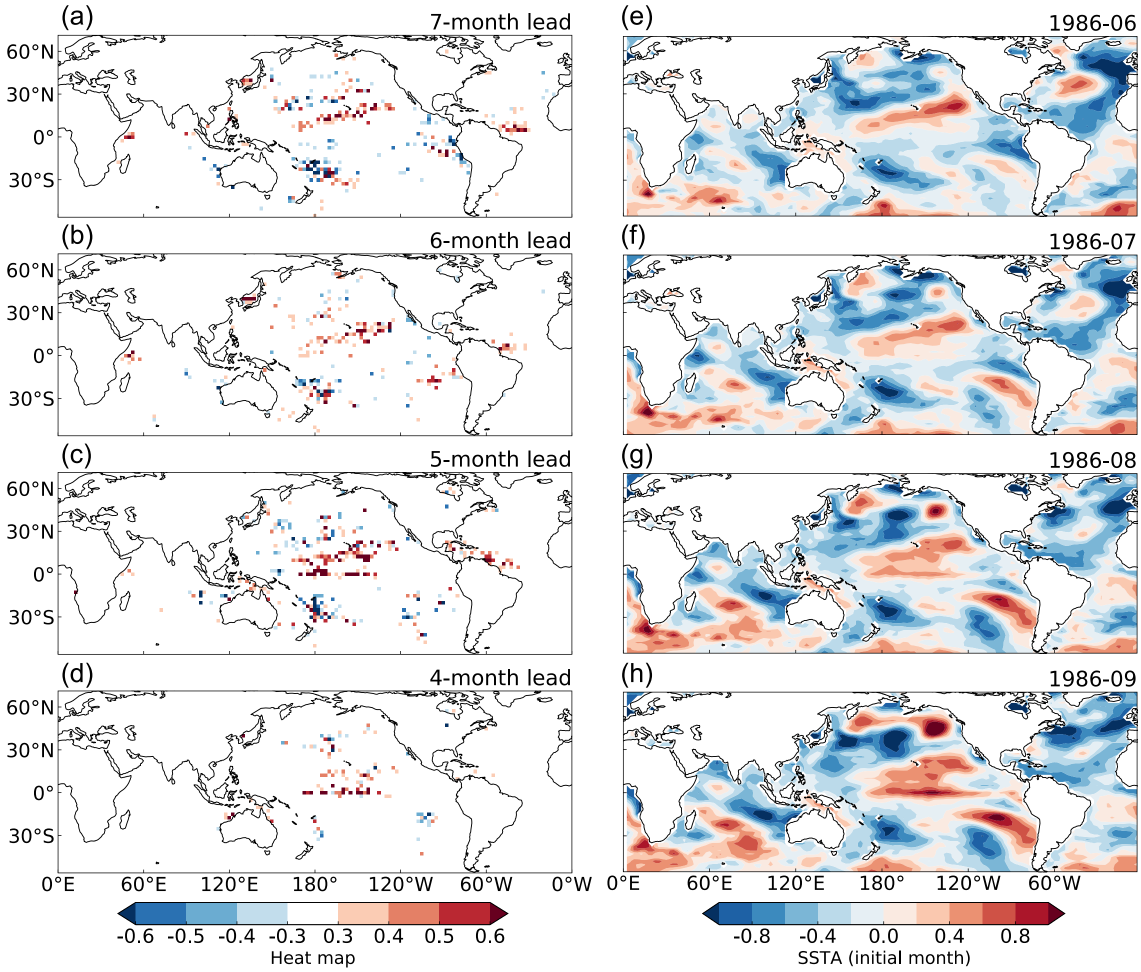

Fig. S9. Attribution heat map of EP El Niño in 1986.

Table S1. Details of CMIP6 models.

Model name	Institution
ACCESS-CM2	CSIRO (Commonwealth Scientific and Industrial Research Organisation, Aspendale), ARCCSS (Australian Research Council Centre of Excellence for Climate System Science)
ACCESS-ESM1-5	CSIRO
BCC-CSM2-MR BCC-ESM1	Beijing Climate Center
CAMS-CSM1-0	Chinese Academy of Meteorological Sciences
CESM2 CESM2-FV2 CESM2-WACCM CESM2-WACCM-FV2	NCAR (National Center for Atmospheric Research, Climate and Global Dynamics Laboratory)
CNRM-CM6-1 CNRM-CM6-1-HR CNRM-ESM2-1	CNRM (Centre National de Recherches Meteorologiques), CERFACS (Centre Europeen de Recherche et de Formation Avancee en Calcul Scientifique)
CanESM5 CanESM5-CanOE	Canadian Centre for Climate Modelling and Analysis, Environment and Climate Change Canada
E3SM-1-0 E3SM-1-1 E3SM-1-1-ECA	LLNL (Lawrence Livermore National Laboratory); ANL (Argonne National Laboratory); BNL (Brookhaven National Laboratory); LANL (Los Alamos National Laboratory); LBNL (Lawrence Berkeley National Laboratory); ORNL (Oak Ridge National Laboratory); PNNL (Pacific Northwest National Laboratory); SNL (Sandia National Laboratories).
FGOALS-f3-L FGOALS-g3	Chinese Academy of Sciences
GFDL-CM4 GFDL-ESM4	National Oceanic and Atmospheric Administration, Geophysical Fluid Dynamics Laboratory
GISS-E2-1-G GISS-E2-1-G-CC GISS-E2-1-H	Goddard Institute for Space Studies
INM-CM4-8 INM-CM5-0	Institute for Numerical Mathematics, Russian Academy of Science
IPSL-CM6A-LR	Institut Pierre Simon Laplace
KACE-1-0-G	National Institute of Meteorological Sciences/Korea Meteorological Administration, Climate Research Division
MIROC-ES2L MIROC6	JAMSTEC (Japan Agency for Marine-Earth Science and Technology), AORI (Atmosphere and Ocean Research Institute, The University of Tokyo), NIES (National Institute for Environmental Studies), and R-CCS (RIKEN Center for Computational Science)
MPI-ESM-1-2-HAM	ETH Zurich; Max Planck Institut fur Meteorologie; Forschungszentrum Julich; University of Oxford; Finnish Meteorological Institute; Leibniz Institute for Tropospheric Research; Center for Climate Systems Modeling (C2SM) at ETH Zurich
MPI-ESM1-2-LR	Max Planck Institute for Meteorology
MRI-ESM2-0	Meteorological Research Institute, Japan
NESM3	Nanjing University of Information Science and Technology
NorCPM1	NorESM Climate modeling Consortium consisting of CICERO (Center for International Climate and Environmental Research), MET-Norway (Norwegian Meteorological Institute), NERSC (Nansen Environmental and Remote Sensing Center), NILU (Norwegian Institute for Air Research), UiB (University of Bergen), UiO (University of Oslo) and UNI (Uni Research, Bergen)
NorESM2-LM NorESM2-MM	NorESM Climate modeling Consortium consisting of CICERO (Center for International Climate and Environmental Research)
SAM0-UNICON	Seoul National University
UKESM1-0-LL	Met Office Hadley Centre; Natural Environment Research Council; National Institute of Meteorological Sciences/Korea Meteorological Administration, Climate Research Division; National Institute of Water and Atmospheric Research

Table S2. Ensemble member numbers of NMME models.

Model name	Ensemble members
COLA-RSMAS-CCSM4	10
GFDL-CM2p1-aer04	10
GFDL-CM2p5-FLOR-A06	10
GFDL-CM2p5-FLOR-B01	10
CanCM4i	10
NCEP-CFSv2	10

Table S3. Percentages for the NMME model of the selected event in calculating the zonal center for each lead month.

Lead (months)	EP El Niño	CP El Niño	EP La Niña	CP La Niña
1	100.0%	87.5%	100.0%	100.0%
2	100.0%	87.5%	100.0%	100.0%
3	100.0%	87.5%	100.0%	100.0%
4	100.0%	87.5%	100.0%	100.0%
5	100.0%	87.5%	100.0%	83.3%
6	100.0%	75.0%	100.0%	66.7%
7	100.0%	75.0%	83.3%	66.7%
8	100.0%	75.0%	83.3%	50.0%
9	100.0%	50.0%	66.7%	50.0%
10	100.0%	50.0%	50.0%	50.0%
11	100.0%	50.0%	66.7%	50.0%

Table S4. Percentages for the CNN model of the selected event in calculating the zonal center for each lead month.

Lead (months)	EP El Niño	CP El Niño	EP La Niña	CP La Niña
1	100.0%	100.0%	100.0%	100.0%
2	100.0%	100.0%	100.0%	100.0%
3	100.0%	100.0%	100.0%	100.0%
4	100.0%	100.0%	100.0%	100.0%
5	100.0%	100.0%	100.0%	100.0%
6	100.0%	100.0%	100.0%	100.0%
7	100.0%	100.0%	83.3%	100.0%
8	100.0%	87.5%	83.3%	100.0%
9	100.0%	100.0%	83.3%	100.0%
10	100.0%	100.0%	83.3%	100.0%
11	75.0%	75.0%	66.7%	100.0%

REFERENCES

Capotondi, A., A. T. Wittenberg, J.-S. Kug, K. Takahashi, and M. J. McPhaden, 2020: ENSO diversity. *El Niño Southern Oscillation in a Changing Climate*, M. J. McPhaden and A. Santoso, Eds., American Geophysical Union, 65–86, https://doi.org/10.1002/9781119548164.ch4.

Freund, M. B., B. J. Henley, D. J. Karoly, H. V. McGregor, N. J. Abram, and D. Dommenget, 2019: Higher frequency of Central Pacific El Niño events in recent decades relative to past centuries. *Nature Geoscience*, **12**, 450–455, https://doi.org/10.1038/s41561-019-0353-3.

Kug, J.-S., F.-F. Jin, and S.-I. An, 2009: Two types of El Niño events: Cold tongue El Niño and warm pool El Niño. *J. Climate*, **22**, 1499–1515, https://doi.org/10.1175/2008JCLI2624.1.

Ren, H.-L., and F.-F. Jin, 2011: Niño indices for two types of ENSO. *Geophys. Res. Lett.*, **38**, L04704, https://doi.org/10.1029/2010GL046031.

Sullivan, A., J.-J. Luo, A. C. Hirst, D. H. Bi, W. J. Cai, and J. H. He, 2016: Robust contribution of decadal anomalies to the frequency of central-Pacific El Niño. *Scientific Reports*, **6**, 38540, https://doi.org/10.1038/srep38540.

Takahashi, K., A. Montecinos, K. Goubanova, and B. Dewitte, 2011: ENSO regimes: Reinterpreting the canonical and Modoki El Niño.

Geophys. Res. Lett., **38**, L10704, https://doi.org/10.1029/2011gl047364.

Wang, L., H.-L. Ren, J. S. Zhu, and B. H. Huang, 2020: Improving prediction of two ENSO types using a multi-model ensemble based on stepwise pattern projection model. *Climate Dyn.*, **54**, 3229−3243, https://doi.org/10.1007/s00382-020-05160-2.

Wang, S.-Y., M. L'Heureux, and H.-H. Chia, 2012: ENSO prediction one year in advance using western North Pacific sea surface temperatures. *Geophys. Res. Lett.*, **39**, L05702, https://doi.org/10.1029/2012GL050909.

Wyrtki, K., 1975: El Niño—The dynamic response of the equatorial Pacific ocean to atmospheric forcing. *J. Phys. Oceanogr.*, **5**, 572−584, https://doi.org/10.1175/1520-0485(1975)005<0572:ENTDRO>2.0.CO;2.

Yeh, S.-W., J.-S. Kug, B. Dewitte, M.-H. Kwon, B. P. Kirtman, and F.-F. Jin, 2009: El Niño in a changing climate. *Nature*, **461**, 511−514, https://doi.org/10.1038/nature08316.

Zhang, H. H., A. Clement, and P. Di Nezio, 2014: The South Pacific meridional mode: A mechanism for ENSO-like variability. *J. Climate*, **27**, 769−783, https://doi.org/10.1175/JCLI-D-13-00082.1.